Shunsuke TAKEMURA[1], Satoru BABA[1], Suguru YABE[2], Kentaro EMOTO[3], Katsuhiko SHIOMI[4], and Takanori MATSUZAWA[4]

[1]Earthquake Research Institute, the University of Tokyo, 1-1-1 Yayoi, Bunkyo-ku, Tokyo 113-0032, Japan

[2]Geological Survey of Japan, National Institute of Advanced Industrial Science and Technology, Tsukuba Central 7, 1-1-1 Higashi, Tsukuba, Ibaraki 305-8567, Japan

[3]Geophysics, Graduate School of Science, Tohoku University, 6-3, Aramaki-aza-aoba, Aoba-ku, Sendai 980-8578, Japan

[4]National Research Institute for Earth Science and Disaster Resilience, 3-1 Tennodai, Tsukuba, Ibaraki 305-0006, Japan

Corresponding author: Shunsuke TAKEMURA (shunsuke@eri.u-tokyo.ac.jp)

Key Points:

- Comprehensive detection and source parameter estimations of shallow very low frequency earthquake swarms along the Nankai Trough.
- The scaling relationship between the activity areas and cumulative moments of the swarms roughly follows $Mo \quad A^{3/2}$.
- Along-strike variations of the scaling law for swarm durations reflect differences in fracture energies of slow earthquakes.

Abstract

We detected shallow very low frequency earthquakes (VLFEs) off the Cape Muroto and Kii Channel in the Nankai subduction zone and estimated their moment rate functions. From the present and previously estimated catalogs, we investigated the along-strike variations of shallow VLFE activity along the Nankai Trough. The along-strike variations could be related to pore fluids and subducted seamounts. We defined the shallow VLFE swarms and investigated the scaling relationships of their cumulative moments, activity area, and durations in each region. Detected swarms were considered candidates for shallow slow slip events. A similar scaling relationship was observed between the cumulative moments and activity areas, irrespective of regions. It indicates similar stress drops in each region. However, the relationship between the cumulative moments and durations varied. This difference was explained by the along-strike variations in the fracture energies of shallow slow earthquakes.

Plain Language Summary

Slow earthquakes are characterized as slips much slower than similar-size regular earthquakes. Although interactions between the shallow slow earthquakes and large tsunamigenic earthquakes have often been discussed, our knowledge of the source characteristics and spatial variations of the shallow slow earthquakes is still limited. In this study, we quantitatively investigated the activity

characteristics of shallow, very low frequency earthquakes (VLFEs) along the Nankai Trough. The relationship between the subducted seamounts and shallow slow earthquake activities was observed to vary. Activity areas and released cumulative moments of shallow VLFE swarms exhibited a similar scaling law irrespective of regions. However, the duration and cumulative moments of the swarms varied in each region. These characteristics can provide key information on the frictional conditions of slow earthquake faults in shallow plate boundaries.

1 Introduction

Regular (fast) and slow earthquakes occur along plate boundaries in subduction zones to release the accumulated stress due to subduction (summarized in Obara & Kato, 2016; Uchida & Bürgmann, 2019). Different slip phenomena are separately distributed on the plate boundaries (e.g., Dixon et al., 2014; Nishikawa et al., 2019; Takemura, Okuwaki, et al., 2020; Vaca et al., 2018). These slips can be captured from geodetic and seismic observations. The total slips of moderate-to-large earthquakes and small repeating earthquakes can be evaluated by geodetic fault modeling (e.g., Hori et al., 2021; Okada, 1992) and empirical relationships between seismic moments and slips (e.g., Nadeau & Johnson, 1998), respectively. However, it is still difficult to evaluate small deformations due to slow slip events (SSEs), which are geodetic slips of slow earthquakes with durations of several days to years. SSEs with *Mw* 5.5 and 6.5 are the detectable limits in onshore and offshore regions, even when using dense Global Navigation Satellite System observations in Japan (e.g., Agata et al., 2019; Nishimura et al., 2013; Suito, 2016).

Slow earthquakes can also be observed at seismic stations. Low frequency earthquakes (LFEs) and tectonic tremors are observed in frequency ranges of 2-8 Hz (e.g., Obara, 2002). Tremors can be considered superpositions of small LFEs (e.g., Shelly et al., 2007). Very low frequency earthquakes (VLFEs) are observed in the lower frequency band (0.02–0.05 Hz) (e.g., Ghosh et al., 2015; Obara & Ito, 2005). When seismic slow earthquake swarms occur simultaneously during SSEs, they are called episodic tremor and slip (ETS; Hirose & Obara, 2006; Rogers & Dragert, 2003). Small swarms of tremors and VLFEs without obvious geodetic signals have often been observed around the world. Such small swarms can be considered proxies of SSEs that have *Mw* smaller than the detectable limits of geodetic observations. Thus, using dense onshore seismic networks, the characteristics of the swarms of deep LFEs and tremors, which occur at deeper extensions of megathrust zones, have been investigated (e.g., Aiken & Obara, 2021; Daiku et al., 2018; Frank & Brodsky, 2019; Passarelli et al., 2021). Empirical relationships between the geodetic moments of SSEs and seismic moments (or energies) of swarms have been proposed for the monitoring of slips on plate boundaries.

Slow earthquakes occur at shallower extensions of megathrust zones in the offshore regions of the Nankai subduction zone (Figure 1). Because very low-frequency surface waves from shallow VLFEs effectively propagate even in onshore regions and the offshore observations are still limited, long-term activities

of shallow VLFEs, especially in Nankai, have been investigated from onshore broadband records (e.g., Baba et al., 2020; Takemura, Matsuzawa, et al., 2019). Takemura et al. (2021) conducted template matching and relocation for shallow VLFEs and evaluated their moment rate functions southeast of the Kii Peninsula, Japan, From the spatial distributions of the cumulative moments of shallow VLFEs, they found a relationship between shallow VLFE activity and the paleo-Zenisu ridge, which subducted southeast off the Kii Peninsula. In this study, we extend our previous work (Takemura et al., 2021) to off the Cape Muroto and Kii Channel to reveal along-strike variations in shallow VLFE activity along the Nankai Trough. We also investigate the source characteristics of shallow VLFE swarms, which are candidates for shallow SSEs, using our new comprehensive moment-rate-function catalog of shallow VLFEs along the Nankai Trough. We compare the cumulative moments of shallow VLFE swarms with the geodetic moments of the corresponding shallow SSEs to discuss slip monitoring on the shallow plate boundary.

2 Data and Methods

We used broadband records from full-range seismograph network stations (F-net; Aoi et al., 2020) that are operated by the National Research Institute for Earth Science and Disaster Resilience (NIED), Japan. To avoid microseismic signals, we used a zero-phase Butterworth filter with frequencies of 0.02–0.05 Hz. The analyzed period in this study ranged from April 2004 to March 2021. The detection and relocation processes of shallow VLFEs were similar to those in Takemura, Noda, et al. (2019) (see Text S1). We divided the study area into three regions: (A) southeast of the Kii Peninsula, (B) south of the Kii Peninsula, and (C) off the Cape Muroto and Kii Channel (dashed rectangles in Figure 1).

After detection and relocation (gray circles in Figure 1), we estimated the moment rate functions of the shallow VLFEs in Region C, which were constructed using a series of 6-s Küpper wavelets. The weights of each Küpper pulse were estimated using a Monte-Carlo-based simulated annealing method (Takemura et al., 2021). The synthetic waveforms from sources with a single 6-s Küpper pulse were evaluated by reciprocal calculations via OpenSWPC (Maeda et al., 2017) using the regional three-dimensional velocity structure model (Koketsu et al., 2012; Takemura, Yabe, et al., 2020; Tonegawa et al., 2017). Other technical details are provided in Text S1. An example of the estimated moment rate function of the shallow VLFEs in Region C is illustrated in Figure S1. The fitness between the observed and synthetic waveforms improved compared to those from the previous catalog (Takemura, Matsuzawa, et al., 2019). We also compared the estimated moment rate function with the velocity waveforms of the tremor band (2–8 Hz) at N.KMTF (Figure S2) and several Hi-net stations (Figure S3). The envelope shapes of tremors typically correlate with the moment rate functions of VLFEs (e.g., Ide et al., 2008; Yabe et al., 2019). Although high-frequency seismograms can be complicated due to small-scale heterogeneities and subducting oceanic plates (e.g., Furumura & Singh, 2002; Takemura et al., 2017), tremor envelopes also have multi-peak packets. This

supports the longer-duration and multi-peak moment rate functions of a shallow VLFE.

After estimating the moment rate function for shallow VLFEs in region C, we combined this catalog with our previous catalog (regions A and B). From new catalog, we detected the shallow VLFE swarms in each region based on the criteria proposed by Kurihara & Obara (2021). First, we evaluated the expected inter-event times in each region by dividing the analysis period (17 y) by the total number of shallow VLFEs in each region. In this study, shallow VLFE swarms were defined as more than ten consequent shallow VLFEs with inter-event times shorter than the expected inter-event time in each region. Examples of shallow VLFE swarms are presented in Figure 2. The shallow VLFE episode from December 2020 was constructed by four shallow VLFE swarms in regions A and B.

After swarm detection, we evaluated the cumulative moment, duration, activity areas, and along-strike spreading distance of each shallow VLFE swarm. The activity areas and along-strike spreading distances were calculated using the convex hull in the Python module (red enclosed area in Figure 2b). To evaluate the cumulative moments and activity areas of the swarms, we used the shallow VLFEs with variance reductions equal to or greater than 30%. It should also be noted that because the along-dip locations of shallow VLFEs have relatively large uncertainties due to station distributions (see Figures 1b and 1d of Takemura, Noda, et al., 2019, and Figure S1 of Takemura et al., 2021), their swarm areas are expected to be overestimated.

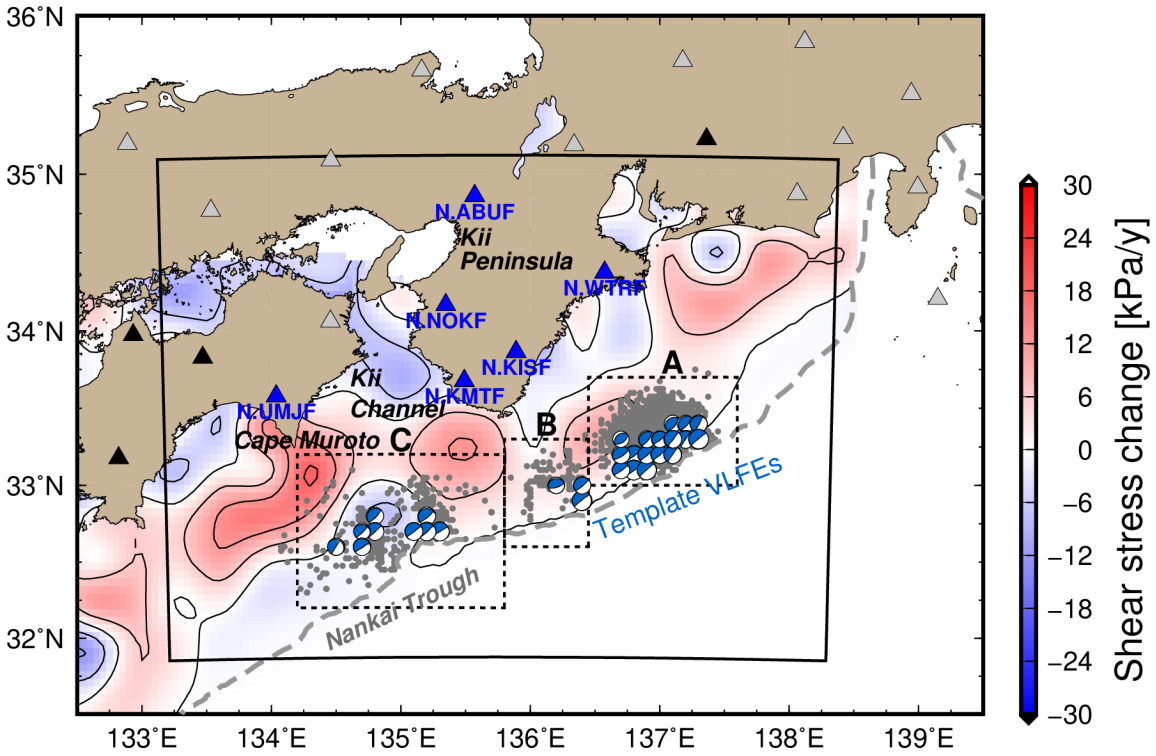

Figure 1. Map of the Nankai region. Blue focal spheres are the template shallow VLFEs, which are well-constrained centroid moment tensor solutions derived from Takemura, Matsuzawa, et al. (2019). Background color in the map represents the shear stress change rate due to subduction of the Philippine Sea Plate (Noda et al., 2018). Gray circles are the epicenters of the detected shallow VLFEs. Shallow VLFEs in regions A and B are from Takemura et al. (2021). Shallow VLFEs in region C are from this study. Triangles denote the F-net stations. Stations with solid black and blue triangles were used for template matching and relocation. Stations represented by solid gray triangles were not used in the analysis. Moment rate function estimates for the detected VLFEs were derived from the data of the solid blue triangles. The black rectangle represents the horizontal calculation region for Green's functions. The gray dashed line represents the deformation front (Nankai Trough).

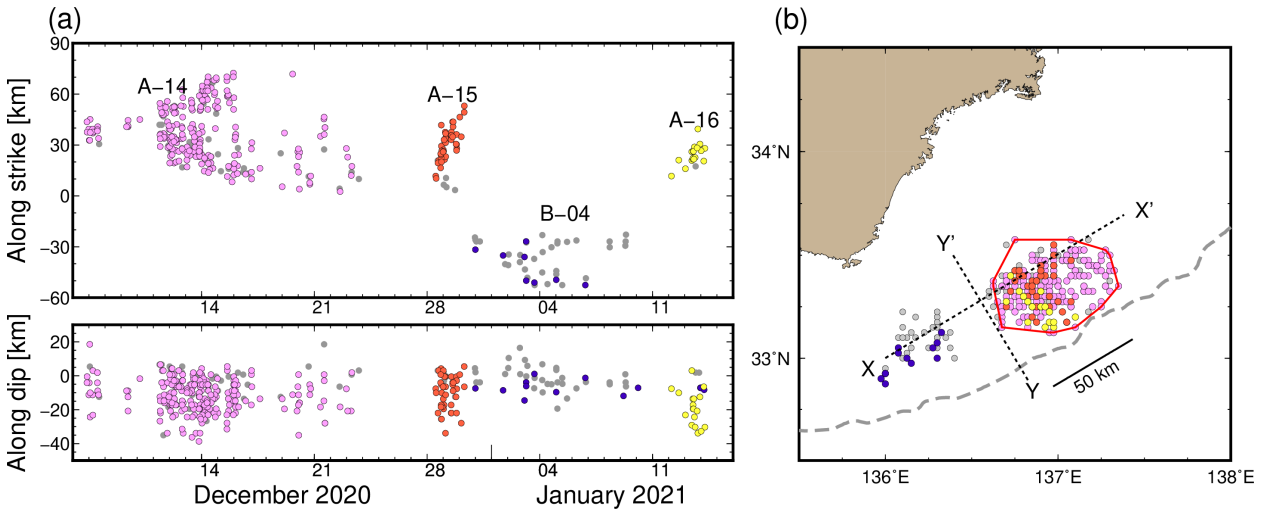

Figure 2. An example of shallow VLFE swarm detection. An example episode occurred in regions A and B from 6 December 2020 to 14 January 2021 (JST). Gray circles represent shallow VLFEs with variance reductions $< 30\%$. (a) Temporal variations of shallow VLFE locations along-strike (X-X') and along-dip (Y-Y'). Colors represent swarm indices. (b) Map view of the shallow VLFE swarms from 6 December 2020 to 14 January 2021. The red enclosed area is the convex-hull of the swarm A-14. The intersection point between X-X' and Y-Y' in (b) represents X = 0 km and Y = 0 km in (a).

3 Results and Discussion

Temporal variation of the cumulative moments of shallow VLFEs along the Nankai Trough is shown in Figure 3a. The blue, purple dotted, and red bold lines represent cumulative moments of shallow VLFEs in regions A, B, and C, respectively. Longitudinal and temporal variations of shallow VLFE activity are shown in Figure 3b. The spatial distribution of cumulative moments of 17 year of shallow VLFEs within $0.05° \times 0.05°$ blocks is shown in Figure 3c. Areas with large cumulative moments were observed in regions A and C, where low S-wave velocity structures have been confirmed around the plate boundary (e.g., Akuhara et al., 2020; Tonegawa et al., 2017; Yamamoto et al., 2017). This indicates rich pore fluid conditions in regions A and C. Subducted seamounts in these regions (Kodaira et al., 2000; Park et al., 2004) are plotted by gray shading areas in Figure 3c. The effects of the presence of subducted seamounts on seismicity have been discussed in various subduction zones (e.g., Chesley et al., 2021; Wang & Bilek, 2014). The relationship between shallow VLFEs and seamounts varied along the Nankai Trough. In region A, the area with larger cumulative moments corresponds to the western edge of the paleo-Zenisu ridge. The stress and structural heterogeneities in the ridge area can promote slow earthquakes (e.g., Takemura et al., 2021; Toh et al., 2020). However, in region C, shallow VLFEs are active on the up-dip side of the subducted seamount.

Numerical studies (e.g., Ruh et al., 2016; Sun et al., 2020) demonstrated that the seamount caused the formation of a stress shadow in its up-dip part and its down-dip surrounding regions. Although the spatial relationships between shallow VLFEs and seamounts vary, the reduction of effective normal stress due to the subducted seamounts and slab-derived fluids can promote shallow earthquakes in regions A and C.

We detected 16, 4, and 9 shallow VLFE swarms in regions A, B, and C, respectively (Table S1, Figure 4). We discarded the A-01 swarm that started on September 6, 2004 (Figure S4) since this swarm might be triggered by the *Mw* 7.4 intraslab earthquake and aftershocks in region A (light blue square in Figure 4). Figure 4a shows the relationship between the cumulative moments and areas of the shallow VLFE swarms. Although along-dip locations of the relocated shallow VLFEs had relatively large uncertainties due to station distributions, the rupture area A approximately follows a scaling law similar to regular earthquakes and deep SSEs ($Mo \quad A^{3/2}$; Gao et al., 2012; Kanamori & Brodsky, 2004). A similar scaling law between the cumulative moments and areas irrespective of the regions indicates that stress drops of the shallow VLFE swarms should be similar in all regions. Regional differences were observed in the relationship between the cumulative moments and durations of the shallow VLFE swarms. The durations of the shallow VLFE swarms in region C were almost one order larger than those in region A. It was recently reported that LFEs, and LFE clusters likely follow $Mo \quad ^3$ rather than Mo (e.g., Aiken & Obara, 2021; Supino et al., 2020). The durations of the shallow VLFE swarms in region A roughly followed $Mo \quad ^3$, rather than $Mo \quad$. The Mo is a typical scaling law of slow earthquake families (Ide et al., 2007). Such studies were difficult in regions B and C because of the insufficient number of shallow VLFE swarms.

Longer durations of shallow VLFE swarms in region C also indicate its slower spreading. Figure 4c shows the relationship between the cumulative moments and apparent spreading speeds, calculated by dividing the along-strike distances by the duration of each swarm. These speeds can be considered as the average along-strike rupture speeds of possible shallow SSEs. The apparent spreading speeds in region A range from 5 to 10 km/day, corresponding to the typical migration speeds of slow earthquakes (e.g., Houston et al., 2011; Obara, 2010). Several rapid (20–30 km/day, like A-15 in Figure 2) spreading have also been confirmed in this study. Shallow VLFE swarms in region C exhibit very slow (~1 km/day) spreading or cluster-like occurrences. The apparent spreading speeds in region B are intermediate between those of regions A and C.

Because the source characteristics of the VLFE swarm correlate with those of the background SSE (e.g., Nakano et al., 2018), the stress drops of shallow SSEs are expected to be similar irrespective of regions (Figure 4a), but the rupture velocities of shallow SSEs are different in the three regions (Figures 4b,c). This difference can be explained by differences in the fracture energies of each region (e.g., Venkataraman & Kanamori, 2004), suggesting differences

in material properties at the plate boundary (e.g., slip weakening distance). Fracture energy also depends on pore fluid pressure. Laboratory experiments show that a small change in the ratio between the average fluid pressure and the average normal stress on the fault can induce a large change in rupture velocity (Passelègue et al., 2020). Tonegawa et al. (2017, 2021) suggested that pore fluid pressure around the plate boundary in region C is expected to be higher than that in region A. Observed differences in the migration velocity may also be caused by such fluid distribution.

To obtain the broadband characteristics of shallow slow earthquakes along the Nankai Trough, we compared the cumulative moments of shallow VLFE swarms with those of corresponding shallow SSEs (Table S2). The cumulative moments of shallow VLFEs were approximately 2–14 % of those of the corresponding shallow SSEs. In contrast, the cumulative moment of deep VLFEs was only 0.1% of the corresponding deep SSEs (e.g., Ito et al., 2009). Passarelli et al. (2021) investigated the seismic productivities of slow earthquakes that were calculated by dividing the cumulative seismic moments of tremors (or earthquake swarms) by the geodetic moments of the corresponding SSEs. It was observed that seismic productivity decreases with increasing depth (Figures 2 and 4 in Passarelli et al., 2021). Daiku et al. (2018) demonstrated the relationship between the seismic productivities of deep ETSs and thermal structures at depths of 30–40 km in the Nankai Trough. Although slow earthquakes in shallow subduction zones were not investigated in both previous studies, differences in seismic productivities between the shallow and deep VLFE swarms in the Nankai Trough can be explained by differences in temperature, which control the frictional and rheological properties of the faults.

A smaller number of shallow SSEs were reported (see Table S2) compared with the deep SSEs (see http://www-solid.eps.s.u-tokyo.ac.jp/~sloweq/; Kano et al., 2018). More shallow SSE fault models will allow us to analyze the quantitative relationship between them and VLFEs. In the future, the statistical characteristics of seismic productivity of shallow slow earthquakes in each region shall be obtained. Consequently, we will quantitatively monitor slips on the shallow plate boundary from seismic slow earthquakes (LFE, tremor, and VLFE).

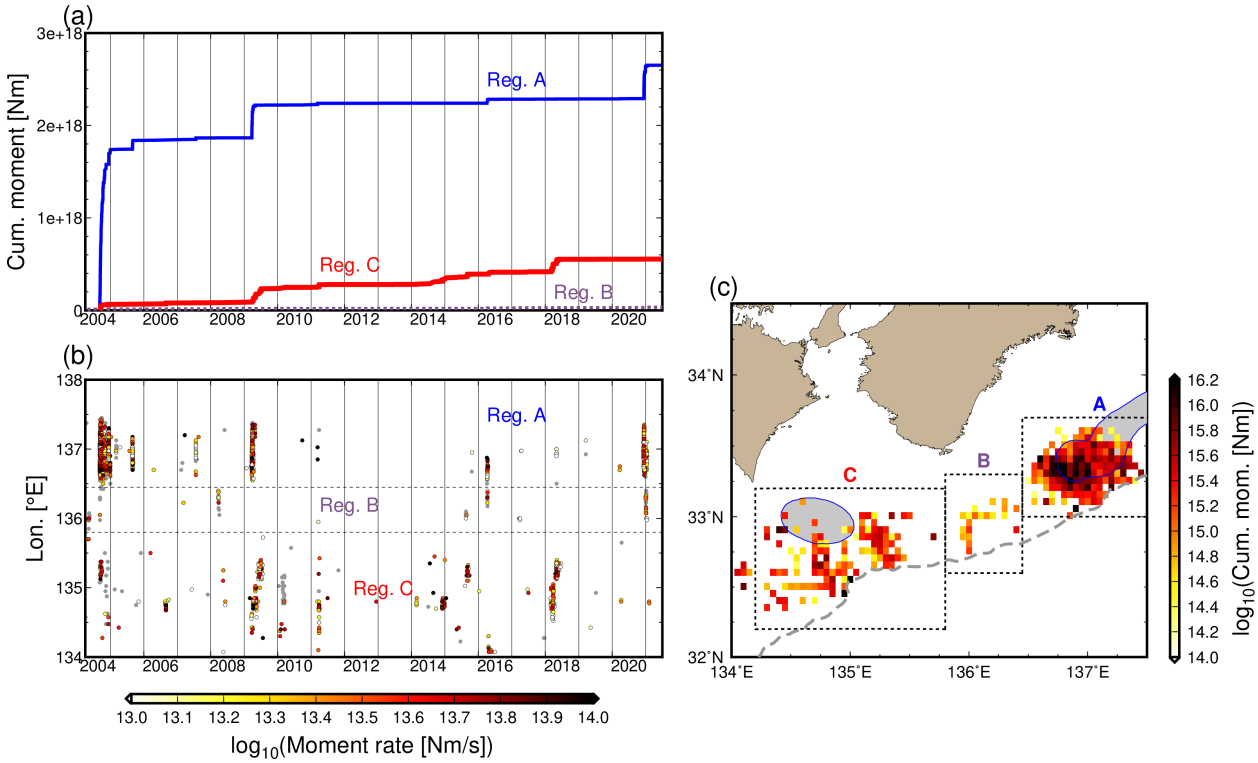

Figure 3. Spatiotemporal variations of 17 y of shallow VLFE data along the Nankai Trough. (a) Temporal variations of the cumulative moments of shallow VLFEs in each region. Blue solid, purple dotted, and red bold lines are cumulative moments of shallow VLFEs in regions A, B, and C, respectively. (b) Temporal variations of the along-strike shallow VLFE activity. The colors of each circle in (b) represent the moment rates of individual shallow VLFEs. (c) Spatial variation of cumulative moments from 17 y of shallow VLFE data. Spatial smoothing of the cumulative number and moments of shallow VLFEs were conducted within the region of 0.05° × 0.05° on the map via the gridding algorithm provided by Generic Mapping Tools (Wessel et al., 2013). The shaded areas represent the subducted seamounts around this region (Kodaira et al., 2000; Park et al., 2004).

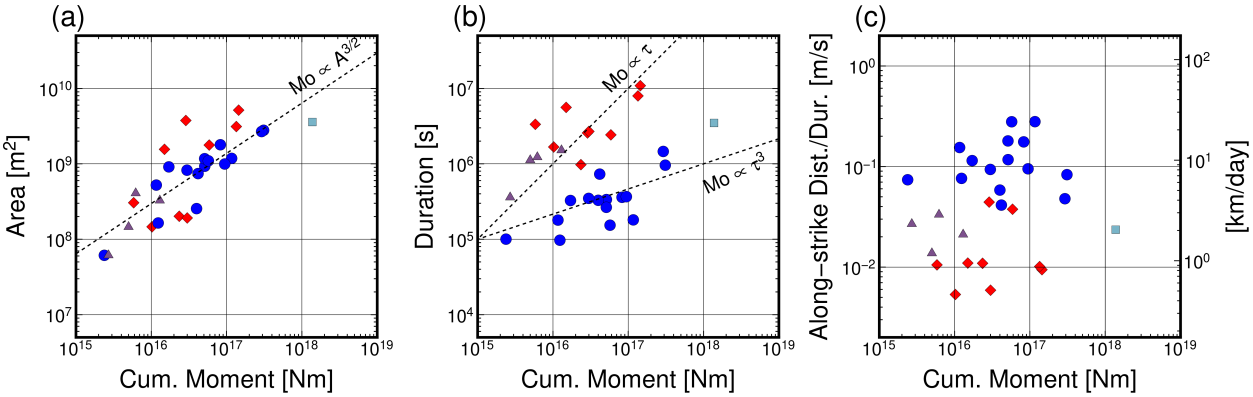

Figure 4. Scaling characteristics of shallow VLFE swarms along the Nankai Trough. Blue circles, purple triangles, and red diamonds are the resultant values in regions A, B, and C, respectively. The light blue square represents the A-01 shallow VLFE swarm that started on September 6, 2004, which can be considered as a triggered VLFE swarm due to the *Mw* 7.4 intraslab earthquake. Cumulative moments versus (a) swarm activity areas, (b) swarm durations, and (c) apparent spreading speeds. The apparent spreading speed was evaluated by dividing the along-strike distance by the duration of each shallow VLFE swarm. Along-strike directions were 239° in regions A and B, and 245° in region C.

5 Conclusions

Using continuous broadband records around the Nankai region, Japan, we revealed the along-strike variations in shallow VLFE activity and source characteristics of shallow VLFE swarms. Shallow VLFEs actively occur off the Cape Muroto, Kii Channel, and southeast off the Kii Peninsula (regions A and C). In region A, large cumulative moments were observed at the western edge of the subducted paleo-Zenisu Ridge. In region C, large moment releases due to shallow VLFEs were confirmed by the up-dip of the subducted seamount. It was inferred that heterogeneous stress and structural properties due to the subducted seamounts promote slow earthquakes along the Nankai Trough.

We investigated the shallow VLFE swarms in each region, which could be candidates for shallow SSEs. We conclude that the cumulative moments and activity areas of shallow VLFE swarms follow a similar scaling law irrespective of region, indicated by similar stress drop values. However, relationships between the cumulative moments and durations of the shallow VLFE swarms vary in each region. The apparent spreading speeds are also variable characteristics. These differences can be explained by regional differences in the fracture energies of the shallow slow earthquakes.

Acknowledgments

Numerical simulations for evaluating the Green's functions were conducted using the Fujitsu PRIMERGY CX600M1/CX1640M1 (Oakforest-PAC) at the In-

formation Technology Center, University of Tokyo. This study was supported by a JSPS KAKENHI Grant-in-Aid for Scientific Research (C), grant number JP21K03696, and a Grant-in-Aid for Scientific Research on Transformative Research Areas "Science of Slow-to-Fast earthquakes," grant numbers JP21H05200, JP21H05203, JP21H05205, and JP21H05206. This study was also supported by ERI JURP 2021-S-B102, which provided the computational resources for calculating the Green's functions.

Data availability statement

The Python package HinetPy (Tian, 2020) was used to download the NIED F-net/Hi-net continuous records (National Research Institute for Earth Science and Disaster Resilience, 2019a, 2019b). We simulated the Green's functions in the local 3D model using OpenSWPC version 5.1.0 https://doi.org/10.5281/zenodo.3982232. The modified 1D layered velocity models of Tonegawa et al. (2017) can be downloaded from https://doi.org/10.5281/zenodo.4158947. The model of Koketsu et al. (2012) was obtained from https://www.jishin.go.jp/evaluation/seismic_hazard_map/lpshm/12_choshuki_dat/. We used the seismic analysis code (Goldstein & Snoke, 2005; Helffrich et al., 2013) and generic mapping tools (Wessel et al., 2013) for signal processing and figure drawing. Data analysis was conducted using NumPy (Harris et al., 2020), SciPy 1.7.0 (https://doi.org/10.5281/zenodo.5000479), and Pandas 1.2.5 (https://doi.org/10.5281/zenodo.5013202). The estimated moment rate functions of shallow VLFEs along the Nankai Trough can be downloaded from https://doi.org/10.5281/zenodo.5211090 and https://doi.org/10.5281/zenodo.5824418.

References

Agata, R., Hori, T., Ariyoshi, K., & Ichimura, T. (2019). Detectability analysis of interplate fault slips in the Nankai subduction thrust using seafloor observation instruments. *Marine Geophysical Research*. https://doi.org/10.1007/s11001-019-09380-y

Aiken, C., & Obara, K. (2021). Data-Driven Clustering Reveals More Than 900 Small Magnitude Slow Earthquakes and Their Characteristics. *Geophysical Research Letters*, *48*(11). https://doi.org/10.1029/2020GL091764

Akuhara, T., Tsuji, T., & Tonegawa, T. (2020). Overpressured Underthrust Sediment in the Nankai Trough Forearc Inferred From Transdimensional Inversion of High-Frequency Teleseismic Waveforms. *Geophysical Research Letters*, *47*(15), 0–3. https://doi.org/10.1029/2020GL088280

Aoi, S., Asano, Y., Kunugi, T., Kimura, T., Uehira, K., Takahashi, N., et al. (2020). MOWLAS: NIED observation network for earthquake, tsunami and volcano. *Earth, Planets and Space*, *72*(1). https://doi.org/10.1186/s40623-020-01250-x

Baba, S., Takemura, S., Obara, K., & Noda, A. (2020). Slow earthquakes illuminating interplate coupling heterogeneities in subduction zones. *Geophysical Research Letters*, 4–5. https://doi.org/10.1029/2020gl088089

Chesley, C., Naif, S., Key, K., & Bassett, D. (2021). Fluid-rich subducting topography generates anomalous forearc porosity. *Nature*, *595*(7866), 255–260. https://doi.org/10.1038/s41586-021-03619-8

Daiku, K., Hiramatsu, Y., Matsuzawa, T., & Mizukami, T. (2018). Slow slip rate and excitation efficiency of deep low-frequency tremors beneath southwest Japan. *Tectonophysics*, *722*(May 2017), 314–323. https://doi.org/10.1016/j.tecto.2017.11.016

Dixon, T. H., Jiang, Y., Malservisi, R., McCaffrey, R., Voss, N., Protti, M., & Gonzalez, V. (2014). Earthquake and tsunami forecasts: Relation of slow slip events to subsequent earthquake rupture. *Proceedings of the National Academy of Sciences*, *111*(48), 17039–17044. https://doi.org/10.1073/pnas.1412299111

Frank, W. B., & Brodsky, E. E. (2019). Daily measurement of slow slip from low-frequency earthquakes is consistent with ordinary earthquake scaling, (October), 1–7.

Furumura, T., & Singh, S. K. (2002). Regional wave propagation from Mexican subduction zone earthquakes: The attenuation functions for interplate and in-slab events. *Bulletin of the Seismological Society of America*, *92*(6), 2110–2125. https://doi.org/10.1785/0120010278

Gao, H., Schmidt, D. A., & Weldon, R. J. (2012). Scaling Relationships of Source Parameters for Slow Slip Events. *Bulletin of the Seismological Society of America*, *102*(1), 352–360. https://doi.org/10.1785/0120110096

Ghosh, A., Huesca-Pérez, E., Brodsky, E., & Ito, Y. (2015). Very low frequency earthquakes in Cascadia migrate with tremor. *Geophysical Research Letters*, *42*(9), 3228–3232. https://doi.org/10.1002/2015GL063286

Goldstein, P., & Snoke, A. (2005). SAC Availability for the IRIS Community. Retrieved from https://ds.iris.edu/ds/newsletter/vol7/no1/193/sac-availability-for-the-iris-community/

Harris, C. R., Millman, K. J., van der Walt, S. J., Gommers, R., Virtanen, P., Cournapeau, D., et al. (2020). Array programming with NumPy. *Nature*, *585*(7825), 357–362. https://doi.org/10.1038/s41586-020-2649-2

Helffrich, G., Wookey, J., & Bastow, I. (2013). *The Seismic Analysis Code*. Cambridge: Cambridge University Press. https://doi.org/10.1017/CBO9781139547260

Hirose, H., & Obara, K. (2006). Short-term slow slip and correlated tremor episodes in the Tokai region, central Japan. *Geophysical Research Letters*, *33*(17), L17311. https://doi.org/10.1029/2006GL026579

Hori, T., Agata, R., Ichimura, T., Fujita, K., Yamaguchi, T., & Iinuma, T. (2021). High-fidelity elastic Green's functions for subduction zone models consistent with the global standard geodetic reference system. *Earth, Planets and Space*, *73*(1). https://doi.org/10.1186/s40623-021-01370-y

Houston, H., Delbridge, B. G., Wech, A. G., & Creager, K. C. (2011). Rapid tremor reversals in Cascadia generated by a weakened plate interface. *Nature Geoscience*, *4*(6), 404–409. https://doi.org/10.1038/ngeo1157

Ide, S., Beroza, G. C., Shelly, D. R., & Uchide, T. (2007). A scaling law for slow earthquakes. *Nature*, *447*(7140), 76–79. https://doi.org/10.1038/nature05780

Ide, S., Imanishi, K., Yoshida, Y., Beroza, G. C., & Shelly, D. R. (2008). Bridging the gap between seismically and geodetically detected slow earthquakes. *Geophysical Research Letters*, *35*(10), 2–7. https://doi.org/10.1029/2008GL034014

Ito, Y., Obara, K., Matsuzawa, T., & Maeda, T. (2009). Very low frequency earthquakes related to small asperities on the plate boundary interface at the locked to aseismic transition. *Journal of Geophysical Research: Solid Earth*, *114*(B11), 1–16. https://doi.org/10.1029/2008JB006036

Kanamori, H., & Brodsky, E. E. (2004). The physics of earthquakes. *Reports on Progress in Physics*, *67*(8), 1429–1496. https://doi.org/10.1088/0034-4885/67/8/R03

Kano, M., Aso, N., Matsuzawa, T., Ide, S., Annoura, S., Arai, R., et al. (2018). Development of a slow earthquake database. *Seismological Research Letters*, *89*(4), 1566–1575. https://doi.org/10.1785/0220180021

Kodaira, S., Takahashi, N., Nakanishi, A., Miura, S., & Kaneda, Y. (2000). Subducted seamount imaged in the rupture zone of the 1946 Nankaido earthquake. *Science*, *289*(5476), 104–106. https://doi.org/10.1126/science.289.5476.104

Koketsu, K., Miyake, H., & Suzuki, H. (2012). Japan Integrated Velocity Structure Model Version 1. *Proceedings of the 15th World Conference on Earthquake Engineering*, 1–4. Retrieved from http://www.iitk.ac.in/nicee/wcee/article/WCEE2012_1773.pdf

Kurihara, R., & Obara, K. (2021). Spatiotemporal Characteristics of Relocated Deep Low-Frequency Earthquakes Beneath 52 Volcanic Regions in Japan Over an Analysis Period of 14 Years and 9 Months. *Journal of Geophysical Research: Solid Earth*, *126*(10). https://doi.org/10.1029/2021JB022173

Maeda, T., Takemura, S., & Furumura, T. (2017). OpenSWPC : An open-source integrated parallel simulation code for mod- eling seismic wave propagation in 3D heterogeneous viscoelastic media.

Nadeau, R. M., & Johnson, J. R. (1998). Seismological Studies at Parkfield IV: Moment Releaase Rates and Estimates of Source Parameters for Small Repeating Earthquakes. *Bull. Seis. Soc. Am.*, *88*(3), 790–814.

Nakano, M., Hori, T., Araki, E., Kodaira, S., & Ide, S. (2018). Shallow very-low-frequency earthquakes accompany slow slip events in the Nankai subduction zone. *Nature Communications*, *9*(1), 984. https://doi.org/10.1038/s41467-018-03431-5

National Research Institute for Earth Science and Disaster Resilience. (2019a). NIED F-net. https://doi.org/10.17598/NIED.0005

National Research Institute for Earth Science and Disaster Resilience. (2019b). NIED Hi-net. https://doi.org/10.17598/NIED.0003

Nishikawa, T., Matsuzawa, T., Ohta, K., Uchida, N., Nishimura, T., & Ide, S. (2019). The slow earthquake spectrum in the Japan Trench illuminated by the S-net seafloor observatories. *Science*, *365*(August), 808–813. https://doi.org/10.1126/science.aax5618

Nishimura, T., Matsuzawa, T., & Obara, K. (2013). Detection of short-term slow slip events along the Nankai Trough, southwest Japan, using GNSS data. *Journal of Geophysical Research: Solid Earth*, *118*(6), 3112–3125. https://doi.org/10.1002/jgrb.50222

Noda, A., Saito, T., & Fukuyama, E. (2018). Slip-Deficit Rate Distribution Along the Nankai Trough, Southwest Japan, With Elastic Lithosphere and Viscoelastic Asthenosphere. *Journal of Geophysical Research: Solid Earth*, *123*(9), 8125–8142. https://doi.org/10.1029/2018JB015515

Obara, K. (2002). Nonvolcanic deep tremor associated with subduction in southwest Japan. *Science*, *296*(5573), 1679–1681. https://doi.org/10.1126/science.1070378

Obara, K. (2010). Phenomenology of deep slow earthquake family in southwest Japan: Spatiotemporal characteristics and segmentation. *Journal of Geophysical Research: Solid Earth*, *115*(8), 1–22. https://doi.org/10.1029/2008JB006048

Obara, K., & Ito, Y. (2005). Very low frequency earthquakes excited by the 2004 off Kii peninsula earthquakes: A dynamic deformation process in the large accretionary prism. *Earth, Planets and Space*, *57*(4), 321–326. https://doi.org/10.1186/BF03352570

Obara, K., & Kato, A. (2016). Connecting slow earthquakes to huge earthquakes. *Science*, *353*(6296), 253–257. https://doi.org/10.1126/science.aaf1512

Okada, Y. (1992). Internal Deformation due to Shear and Tensile Faults in a Half-space. *Bulletin of the Seismological Society of America*, *82*(2), 1018–1040.

Park, J.-O., Moore, G. F., Tsuru, T., Kodaira, S., & Kaneda, Y. (2004). A subducted oceanic ridge influencing the Nankai megathrust earthquake rupture. *Earth and Planetary Science Letters*, *217*(1–2), 77–84. https://doi.org/10.1016/S0012-821X(03)00553-3

Passarelli, L., Selvadurai, P. A., Rivalta, E., & Jónsson, S. (2021). The source scaling and seismic productivity of slow slip transients. *Science Advances*, *7*(32). https://doi.org/10.1126/sciadv.abg9718

Passelègue, F. X., Almakari, M., Dublanchet, P., Barras, F., Fortin, J., & Violay, M. (2020). Initial effective stress controls the nature of earthquakes. *Nature Communications*, *11*(1), 1–8. https://doi.org/10.1038/s41467-020-18937-0

Rogers, G., & Dragert, H. (2003). Episodic tremor and slip on the Cascadia subduction zone: the chatter of silent slip. *Science*, *300*(5627), 1942–1943. https://doi.org/10.1126/science.1084783

Ruh, J. B., Sallarès, V., Ranero, C. R., & Gerya, T. (2016). Crustal deformation dynamics and stress evolution during seamount subduction: High-resolution 3-D numerical modeling. *Journal of Geophysical Research: Solid Earth*, *121*(9), 6880–6902. https://doi.org/10.1002/2016JB013250

Shelly, D. R., Beroza, G. C., & Ide, S. (2007). Non-volcanic tremor and low-frequency earthquake swarms. *Nature*, *446*(7133), 305–307. https://doi.org/10.1038/nature05666

Suito, H. (2016). Detectability of Interplate Fault Slip around Japan, Based on GEONET Daily Solution F3 (in Japanese with English abstract). *Journal of the Geodetic Society of Japan*, *62*(3), 109–120. https://doi.org/10.11366/sokuchi.62.109

Sun, T., Saffer, D., & Ellis, S. (2020). Mechanical and hydrological effects of seamount subduction on megathrust stress and slip. *Nature Geoscience*, *13*(March). https://doi.org/10.1038/s41561-020-0542-0

Supino, M., Poiata, N., Festa, G., Vilotte, J. P., Satriano, C., & Obara, K. (2020). Self-similarity of low-frequency earthquakes. *Scientific Reports*, *10*(1), 1–9. https://doi.org/10.1038/s41598-020-63584-6

Takemura, S., Kobayashi, M., & Yoshimoto, K. (2017). High-frequency seismic wave propagation within the heterogeneous crust: effects of seismic scattering and intrinsic attenuation on ground motion modelling. *Geophysical Journal International*, *210*(3), 1806–1822. https://doi.org/10.1093/gji/ggx269

Takemura, Shunsuke, Noda, A., Kubota, T., Asano, Y., Matsuzawa, T., & Shiomi, K. (2019). Migrations and Clusters of Shallow Very Low Frequency Earthquakes in the Regions Surrounding Shear Stress Accumulation Peaks Along the Nankai Trough. *Geophysical Research Letters*, *46*(21), 11830–11840. https://doi.org/10.1029/2019GL084666

Takemura, Shunsuke, Matsuzawa, T., Noda, A., Tonegawa, T., Asano, Y., Kimura, T., & Shiomi, K. (2019). Structural Characteristics of the Nankai Trough Shallow Plate Boundary Inferred From Shallow Very Low Frequency Earthquakes. *Geophysical Research Letters*, *46*(8), 4192–4201. https://doi.org/10.1029/2019GL082448

Takemura, Shunsuke, Okuwaki, R., Kubota, T., Shiomi, K., Kimura, T., & Noda, A. (2020). Centroid moment tensor inversions of offshore earthquakes using a three-dimensional velocity structure model: slip distributions on the plate boundary along the Nankai Trough. *Geophysical Journal International*, *222*(2), 1109–1125. https://doi.org/10.1093/gji/ggaa238

Takemura, Shunsuke, Yabe, S., & Emoto, K. (2020). Modelling high-frequency seismograms at ocean bottom seismometers: effects of heterogeneous structures on source parameter estimation for small offshore earthquakes and shallow low-frequency tremors. *Geophysical Journal International*, *223*(3), 1708–1723. https://doi.org/10.1093/gji/ggaa404

Takemura, Shunsuke, Obara, K., Shiomi, K., & Baba, S. (2021). Spatiotemporal variations of shallow very low frequency earthquake activity southeast off the Kii Peninsula, along the Nankai Trough, Japan. *ESSOAr*. https://doi.org/10.1002/essoar.10507824.2

Tian, D. (2020). HinetPy: A Python package to request and process seismic waveform data from Hi-net. https://doi.org/10.5281/zenodo.3885779

Toh, A., Chen, W. J., Takeuchi, N., Dreger, D. S., Chi, W. C., & Ide, S. (2020). Influence of a Subducted Oceanic Ridge on the Distribution of Shallow VLFEs in the Nankai Trough as Revealed by Moment Tensor Inversion and Cluster Analysis. *Geophysical Research Letters*, *47*(15), 0–3. https://doi.org/10.1029/2020GL087244

Tonegawa, T., Araki, E., Kimura, T., Nakamura, T., Nakano, M., & Suzuki, K. (2017). Sporadic low-velocity volumes spatially correlate with shallow very low frequency earthquake clusters. *Nature Communications*, *8*(1), 2048. https://doi.org/10.1038/s41467-017-02276-8

Tonegawa, T., Takemura, S., Yabe, S., & Yomogida, K. (2021). Fluid migration before and during slow earthquakes in the shallow Nankai subduction zone. *Earth and Space Science Open Archieve* . https://doi.org/10.1002/essoar.10508646.1

Uchida, N., & Bürgmann, R. (2019). Repeating Earthquakes. *Annual Review of Earth and Planetary Sciences*, *47*(1), 305–332. https://doi.org/10.1146/annurev-earth-053018-060119

Vaca, S., Vallée, M., Nocquet, J. M., Battaglia, J., & Régnier, M. (2018). Recurrent slow slip events as a barrier to the northward rupture propagation of the 2016 Pedernales earthquake (Central Ecuador). *Tectonophysics*, *724–725*(November 2017), 80–92. https://doi.org/10.1016/j.tecto.2017.12.012

Venkataraman, A., & Kanamori, H. (2004). Observational constraints on the fracture energy of subduction zone earthquakes. *Journal of Geophysical Research: Solid Earth*, *109*(5). https://doi.org/10.1029/2003JB002549

Wang, K., & Bilek, S. L. (2014). Invited review paper: Fault creep caused by subduction of rough seafloor relief. *Tectonophysics*, *610*, 1–24. https://doi.org/10.1016/j.tecto.2013.11.024

Wessel, P., Smith, W. H. F., Scharroo, R., Luis, J., & Wobbe, F. (2013). Generic mapping tools: Improved version released. *Eos*, *94*(45), 409–410. https://doi.org/10.1002/2013EO450001

Yabe, S., Tonegawa, T., & Nakano, M. (2019). Scaled Energy Estimation for Shallow Slow Earthquakes. *Journal of Geophysical Research: Solid Earth*, *124*(2), 1507–1519. https://doi.org/10.1029/2018JB016815

Yamamoto, Y., Takahashi, T., Kaiho, Y., Obana, K., Nakanishi, A., Kodaira, S., & Kaneda, Y. (2017). Seismic structure off the Kii Peninsula, Japan, deduced from passive- and active-source seismographic data. *Earth and Planetary*

Science Letters, *461*, 163–175. https://doi.org/10.1016/j.epsl.2017.01.003